Dynamic 3D deployment of autonomous navigation UAVs for mobile sensors in the Internet of Things

Yang Zhang[1,a], Binbin Wu[2,b], Jie Lu[1,c], Jingzhou Yang[1,d,*]

[1] *CETC Next-generation Mobile Communication Innovation Center, Shanghai, 200331, China*
[2] *College of Communications Engineering, Army Engineering University of PLA, Nanjing, 210007, China*
[a] *zhoulingzi@hotmail.com,* [b] *wbb919@126.com,* [c] *5950458292@126.com,* [d] *heroyjz@163.com*
*Corresponding author

Abstract: *Aiming at the problem of low coverage caused by the difficulty of obtaining the optimal deployment position in existing commonly used distributed deployment algorithms, this paper proposes a three-dimensional (3D) deployment algorithm for Unmanned Aerial Vehicles (UAV) based on potential game. Firstly, a local mutually beneficial game model is designed, and proved the existence of exact potential games and Nash equilibrium in this game model, and the Nash equilibrium solution corresponds to the maximum coverage. Secondly, inspired by the idea of exploration, a solution method based on exploration-based automatic learning machine was designed, and the maximum utility function value of multiple step sizes in the exploration direction is used to update the action selection probability, ensuring the optimal deployment position in each decision cycle. Simulation results show that the proposed distributed deployment algorithm has higher coverage than existing commonly used methods.*

Keywords: *Data collection, UAV, Three-dimensional deployment, Motion planning*

1. Introduction

1.1. Background

The flexibility and mobility of Unmanned Aerial Vehicle (UAV) have been widely concerned and studied for future communication system [1]–[3]. It can be used as an auxiliary means to expand and supplement the ground communication network. Data collection over wireless sensor networks (WSNs) is considered one of the crucial applications for unmanned aerial vehicles (UAVs) and has been extensively studied by researchers [4]. In conventional approaches, wireless sensor nodes (SNs) positioned in various regions transmit their sensing data to a fusion center using different power levels based on their respective distances from the fusion center. Consequently, this variation in energy consumption rates among the sensor nodes can significantly limit the lifetime of wireless sensor networks (WSNs) [5], [6]. To address the limited lifetime issue in WSNs caused by the disparate energy consumption rates, alternative strategies have been explored. One approach involves employing adaptive power control algorithms that dynamically adjust the transmit power of SNs based on their distance to the fusion center. By optimizing the power levels, this technique aims to achieve a more balanced energy distribution among the sensor nodes [7], [8]. Another solution is to implement energy-efficient routing protocols that consider both the energy levels of SNs and their proximity to the fusion center when selecting paths for data transmission. This way, nodes with higher energy reserves can be strategically utilized to relay data from distant SNs, thereby reducing overall energy consumption and extending network lifetime [9], [10]. Furthermore, advancements in harvesting ambient energy sources such as solar or wind power can be leveraged to recharge sensor nodes. Integrating energy harvesting mechanisms into WSNs allows for prolonged operation without relying solely on limited onboard battery capacities [11], [12]. By adopting these approaches and exploring novel techniques, researchers aim to mitigate the energy imbalance issue in WSNs and enhance their longevity for efficient data collection applications using UAVs [13], [14].

1.2. Prior Work

The previous research of UAV mainly focused on the level of control theory and methods. The three-dimensional deployment of unmanned aerial vehicles (UAVs) addresses a crucial challenge in UAV communication. By enabling adjustable flight altitudes and mobility, it offers additional degrees of freedom for effective deployment [15]–[17]. However, this type of deployment also presents challenges

related to the deployment environment, user location and distribution, and the characteristics of the UAV communication channel. These factors need to be carefully considered to achieve optimal deployment in the three-dimensional space for UAVs [18]. With the rapid development of UAV communication technology, there are more and more researches on the communication control combine with flight control [19]. Compared with the traditional fixed node communication on the ground, the mobility and flexibility of UAV can effectively improve the performance of UAV communication system. Although the flexible deployment of UAVs, natural line-of-sight channels and controllable trajectories have brought huge gains to the UAV communication network. However, for the data collection task of ground mobile sensor nodes, the offline deployment algorithm cannot guarantee the coverage and data collection volume of the UAV [20] to the ground sensor nodes in real time. Once the ground sensor nodes leave the effective communication coverage area of the UAV, the correctly demodulated data cannot be collected. Reference [21] proposes that the deployment based on the Grey Wolf algorithm can effectively maximize the average throughput rate of ground users. Reference [22] uses particle swarm optimization to optimize coverage and user communication and rate respectively. However, the traditional centralized optimization algorithm used in these studies is not only computationally intensive, but also does not consider the real-time mobile ground sensor scene.

1.3. Contributions and Organization

This paper constructs a game theory model based on distribution, and proposes an automatic learning algorithm based on exploration to solve the equilibrium solution. The main contents and contributions are as follows:

(1) According to the characteristics of UAV communication channel. Take the signal-to-noise ratio threshold and the maximum number of users served by the UAV as the conditions for the ground sensor node to access the UAV.

(2) The dynamic game model of UAV as a participant is designed and the game is decomposed into sub-games at each time. At the same time, we designed the multi-dimensional discrete action space and the utility function of each player. The utility function takes the number of users accessed by the UAV itself and the number of users accessed by the neighbor UAV into account.

(3) In each sub-game stage, in order to solve the limitations of actions in the discrete action space, we designed the expected actions based on exploration.

2. System Model and Problem Formulation

Considering that low-power sensor equipment is randomly scattered in the mission area, when the UAV group flies to the mission area, the control signal is sent to the ground low-power sensor equipment to access the UAV network for data reporting. It is specified that each low-power sensor device can only be connected to one UAV and needs to meet the channel quality requirements at the same time.
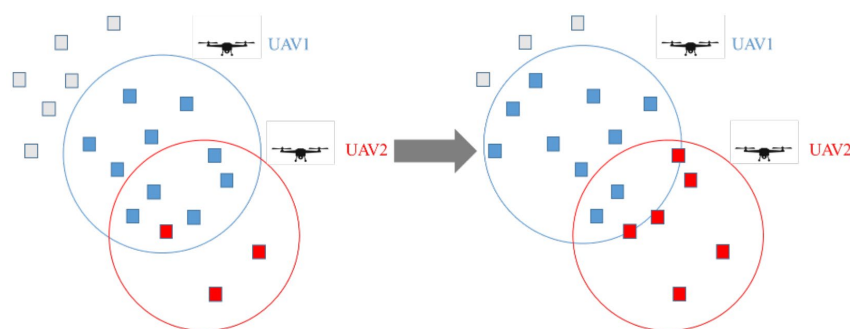

Figure 1: Changes in access sensors during local mutual benefit games.

2.1. Unmanned Data Acquisition Channel Model

The paper size must be set to A4 (210x297 mm). The margins must be set as the following:

UAV data collection channels are ground-air channels, which can be generally divided into LOS, NLOS and multipath fading channels [23], [24]. Although there are many in-depth studies on UAV

communication channels, for example, considering the reflection of ground obstacles and roadside obstacles. Reference [25] designed a three-dimensional channel model based on geometric methods. In the deployment coverage scenario of data collection UAV studied in this paper, the LOS channel is mainly considered, and the power gain within the coverage radius is defined as

$$h(d) = \frac{\beta_0}{H^2 + d^2} \tag{1}$$

Where β_0 is the power gain of per meter, H is the flight altitude of the UAV, d is the distance from the UAV projection position to the ground sensor node, $0 \le d \le d_{\max}$, $d_{\max}$ is the maximum coverage radius of the UAV. The maximum coverage radius is calculated based on the pitch angle and flight altitude of the UAV:

$$d_{\max} = H tan\Phi \tag{2}$$

Let the set of UAV groups defined as U=$\{1,2\cdots U\}$, the set of ground sensors defined as S=$\{1,2\cdots,S\}$, and the mission area be set as a cube model $\Omega = \{\mathbf{p} = (x,y,z) | \mathbf{p}_{down} \prec \mathbf{p} \prec \mathbf{p}_{up}\}$, where $\mathbf{p}_{down}$ is the lower boundary of the area and $\mathbf{p}_{up}$ is the upper boundary. We can set the position of the UAV $\mathbf{p}_{UAV} \in \Omega$ the position of the ground sensor $\mathbf{p}_{SN} \in \Omega$. According to the number of UAVs that meet the coverage requirements, set the rate r_{min} to meet the minimum communication needs of users. The available communication bandwidth for the UAV is B, and the bandwidth utilization efficiency is η. Therefore, we can calculate the number of users that each UAV can serve as $U_{cover} = \lceil \eta B / r_{\min} \rceil$, where $\lceil \cdot \rceil$ indicates rounding up. The approximate number of UAVs required $U = \lceil S/U_{cover} \rceil$, based on the total number of ground sensors can be determined at the same time. A sensor successfully access a UAV requires meeting communication quality requirements $r \ge r_{\min}$, where r is the communication rate of data reported by the sensor.

$$r_{s,u} = \eta B_s \log_2 \left(1 + \frac{p_s h(d_{s,u})}{\sigma^2} \right) \tag{3}$$

Where $B_s = \lceil B/U_{cover} \rceil$ is the maximum bandwidth that the sensor s-th can use, p_s is the transmission power of the s-th sensor, $h(d_{s,u})$ is the channel gain between the s-th sensor and the u-th UAV, $d_{s,u}$ is the distance between the s-th sensor and the u-th UAV. $r_{s,u}$ is the instantaneous communication rate between the s-th sensor and the u-th UAV, and σ^2 is the power of additive Gaussian white noise.

2.2. Deployment Problem Customization

As a three-dimensional deployment of UAV assisted data collection, we take the total number of sensors successfully connected to the UAV as the optimization goal, which can be expressed as:

$$
\begin{aligned}
(P1): \quad &\max_{\mathbf{p}_1\cdots\mathbf{p}_U} \sum_{u=1}^{U}\sum_{s=1}^{S} \text{Access}_{U\times S} \\
s.t. \quad &\mathbf{p}_u = \mathbf{p}_u^{init}, u \in U \\
&\sum_{u=1}^{U} \text{Access}_{U\times S} \le U_{cover} \\
&\sum_{s=1}^{S} \text{Access}_{U\times S} \le 1 \\
&\text{Access}(u,s) = \begin{cases} 1, r_{u,s} \ge r_{\min} \\ 0, other \end{cases} u \in U, s \in S \\
&\mathbf{p}_u \in \Omega, u \in U
\end{aligned}
\tag{4}
$$

The variable $\mathbf{p}_1,\cdots,\mathbf{p}_U$ is the three-dimensional coordinate position of the UAV, and the indicator

matrix $\text{Access}_{U \times S}$ representing the u-th row and s-th column sensors accessed to the UAV in the optimization target, hereinafter referred to as the access matrix. The first constraint is the initial position constraint of the UAV. The second constraint indicates that the number of sensors successful accessed to UAV needs to be less than or equal to the maximum number of service users U_{cover}. The third constraint indicates that each sensor can only access one UAV at most and cannot repeatedly access other UAV. The forth constraint is a communication requirement to ensure the quality of sensor data transmission. The last constraint is a boundary constraint, and the UAV must be within the mission area.

3. Three-Dimensional Deployment Algorithm

3.1. Game Model

Game theory can be divided into two categories, namely cooperative games and non cooperative games according to whether participants have reached a binding cooperation agreement. In general, the information interaction cost of cooperative games is much greater than that of non cooperative games. The key issue in non cooperative game research is how participants choose strategies and make choices that maximize their own benefits when their interests or returns interact. The three elements of the game model are as follows:

$$\mathcal{G} = \left[\mathrm{U}, \{\mathbf{p}_u\}_{u \in \mathrm{U}}, \{f_u\}_{u \in \mathrm{U}} \right] \tag{5}$$

(1) Participant: $\mathrm{U} = \{1, 2 \cdots U\}$ represents a collection of all UAVs that perform data collection tasks.

(2) Strategy space: $\mathrm{A} = \{a_1, a_2, \cdots, a_U\}$ represents the action space selected by the display UAV. For any $u \in \mathrm{U}$, a_u represents the selected action of the u-th UAV, and for $a_u \in \mathrm{A}$, where A is a set of actions.

(3) Utility function: In the UAV assisted data collection and deployment problem, the goal of each UAV is to maximize its own utility function.

3.2. Utility Function Design

In traditional game models, game participants always make decisions based on their own interests, that means participants only considering the maximum individual's utility function. However, in the optimization problem P1, the number of sensors that each UAV can access is limited. When UAVs only consider maximizing their own utility function, their decision-making will fall into a dead cycle, making it difficult to ensure global optimization. In order to improve the performance of game models and be inspired by local mutually beneficial behavior in nature, this chapter proposes a local mutually beneficial game based UAV deployment. The local mutually beneficial behavior in nature refers to the fact that biological individuals consider other individuals of their neighbors when making decisions [26]. Therefore, the utility function in a locally mutually beneficial game is defined as follows:

$$f_u(a_u, a_{J_u}) = g_u\left(a_u, a_{J_u}\right) + \sum_{u' \in J_u} g_{u'}\left(a_{u'}, a_{J_{u'}}\right) \tag{6}$$

Where J_u is the neighbor UAV set of u-th UAVs, which defines the one hop reachable node in the UAV network as the neighbor node. $g_u(a_u, a_{J_u})$ is the number of sensors accessed by the u-th UAV, with a maximum value of U_{cover}, and its expression is as

$$g_u\left(a_u, a_{J_u}\right) = \begin{cases} U_{\text{cover}}, \sum\limits_{s} \text{Access}(\mathrm{u}, \mathrm{s}) > \mathrm{U}_{\text{cover}} \\ \sum\limits_{s} \text{Access}(\mathrm{u}, \mathrm{s}), others \end{cases} \tag{7}$$

Where $\text{Access}(\mathrm{u}, \mathrm{s})$ is the access indication of the s-th sensor to the u-th UAV, which generally follows the constraints in question P1 in the game model. Therefore, when a UAV makes a motion decision at the next moment, it not only considers itself, but also considers its neighbor users. This can prevent a UAV from falling into a dead cycle when reaching its optimal capacity. Based on the above utility function, the local mutual benefit game model can be expressed as:

$$(\mathcal{G}1) = \max_{a_u \in A} f_u\left(a_u, a_{J_u}\right), \forall u \in U \tag{8}$$

Where A is the action set of UAV. Considering that the decision-making actions of UAV at each moment during the deployment process are discrete. We can set fixed length movement values like Δ on each dimension, the action space can be represented as:

$$A = \begin{cases} (0,0,0); (0,0,\Delta); (0,\Delta,0); \\ (0,\Delta,\Delta); (\Delta,0,0); (\Delta,0,\Delta); \\ (\Delta,\Delta,0); (\Delta,\Delta,\Delta); (0,0,-\Delta); \\ (0,-\Delta,0); (0,-\Delta,-\Delta); (-\Delta,0,0); \\ (-\Delta,0,-\Delta); (-\Delta,-\Delta,0); (-\Delta,-\Delta,-\Delta); \\ (-\Delta,-\Delta,\Delta); (-\Delta,\Delta,-\Delta); (-\Delta,\Delta,\Delta); \\ (\Delta,-\Delta,-\Delta); (\Delta,-\Delta,\Delta); (\Delta,\Delta,-\Delta); \\ (\Delta,0,-\Delta); (\Delta,-\Delta,0); (0,\Delta,-\Delta); \\ (0,-\Delta,\Delta); (-\Delta,0,\Delta); (-\Delta,\Delta,0); \end{cases} \tag{9}$$

There are 27 basic motion components in the motion space of UAV, including stationary motion. The UAV selects an action to perform during each decision cycle to track sensors. In order to illustrate the mechanism of local mutually beneficial games.

3.3. Nash Equilibrium Analysis

Then we can know that this game is an exact potential energy game. Alternatively, in precise potential energy games, the amount of change in the utility function caused by any user unilaterally changing their strategy is the same as the amount of change in the potential energy function. At the same time, the theorem that Nash equilibrium is an exact potential energy game is as follows:

Theorem 1. A local mutual benefit game $\mathcal{G}1$ is an exact potential energy game with at least one pure strategy Nash equilibrium solution. In addition, the optimal solution to the problem of maximizing the deployment and access of UAV assisted data collection P1 is the pure strategy Nash equilibrium of the game.

Proof of Theorem 1. First, construct the following potential energy function:

$$\phi(a_u, a_{-u}) = \sum_u f_u(a_u, a_{J_u}) \tag{10}$$

If any UAV changes its action selection from a_u to a'_u, the amount of change in the user's utility function is as follows:

$$\begin{aligned} &\phi(a_u, a_{-u}) \text{-} \phi(a'_u, a_{-u}) \\ &= \sum_u f_u(a_u, a_{J_u}) \text{-} \sum_u f_u(a'_u, a_{J_u}) \\ &= f_u(a_u, a_{J_u}) + \sum_{u' \in J_u} f_{u'}(a_{u'}, a_{J_{u'}}) \\ &\quad - f_u(a'_u, a_{J_u}) - \sum_{u' \in J_u} f_u(a_{u'}, a_{J_{u'}}) \\ &= f_u(a_u, a_{J_u}) - f_u(a'_u, a_{J_u}) \\ &= f_u(a_u, a_{-u}) - f_u(a'_u, a_{-u}) \end{aligned} \tag{11}$$

Based on the above analysis, it can be seen that a unilateral change by any user results in an equal change in the utility function and potential energy function of the UAV. Therefore we can make a

conclusion that a local mutual benefit game is an accurate potential energy game, and its potential energy function is the global number of user accesses.

Accurate potential energy games have many unique properties as follows [27]:

(1) Any precise potential energy game has at least one pure strategic Nash equilibrium;

(2) The global or local optimal solution of the potential energy function is a Nash equilibrium.

3.4. Exploratory Based Stochastic Learning Automata

Firstly, we need to expand the game model from pure strategy to mixed strategy. Note that the mixed strategy distribution vector of the u-th UAV during the i-th iteration is $\mathbf{q}(i) = \big(\mathbf{q}_1(i), \cdots, \mathbf{q}_U(i)\big)$. Where $\mathbf{q}_u(i) \in \triangle(A_u)$, $\triangle(A_u)$ represents the probability distribution set of the u-th UAV in the strategy space AA_u, where $\mathbf{q}_u(i) = (q_{u1}, \cdots, q_{uM})$ is the probability vector for the u-th UAV to select actions, and M is the number of actions in the action space. q_{um} means the probability that the u-th UAV selects the m-th action. Note $h_{um}(\mathbf{q})$ the average utility function that the u-th UAV can obtain when it selects m-th channel($a_u = A(m)$) and other UAVs use a hybrid strategy,

$$h_{um}(\mathbf{q}) = \sum_{a_k, k \neq u} f_u\big(a_1, \cdots, A(m), a_{u+1}, \cdots, a_U\big) \prod_{k \neq u} q_{ka_k} \qquad (12)$$

Inspired by a distributed learning algorithm based on Stochastic Learning Automata (SLA) [28], [29], which is applied to study the random stability of social networks. In sparse data assisted data collection scenarios, the range of sensor distribution is relatively wide, and limited by the maximum flight capacity of UAV, the maximum movement distance in a decision cycle may not have any change in sensor coverage. Therefore, in this sparse scenario, it is difficult for traditional algorithms to solve the Nash equilibrium solution. We redesigned the action space of the game model, set a fixed length movement value $\triangle$ to indicate the movement direction of the UAV, and set the maximum movement distance of the UAV $d_{\max}$ in a decision-making cycle. Based on the above theorem, after the UAV selects an action based on the action selection probability as the direction of movement of the UAV on this side. In this direction, start exploring from the current position of the UAV, and set the maximum exploration range $d_{\max}^e$. Therefore, we can search on a line segment $l_u = (1 - \lambda)\mathbf{p}_u + \lambda A(a_u)d_{\max}^e$, where λ is the search accuracy. We calculate the utility function value at each discrete point on the line segment and take the coordinates at the maximum position $\mathbf{p}_u^{\max}$. The distance d between $\mathbf{p}_u^{\max}$ and $\mathbf{p}_u$ is calculated as the UAV will move in the direction during the next decision cycle. If $d \geq d_{\max}$ then we set $d = d_{\max}$.

Algorithm 1	Exploratory Based Stochastic Learning Automata (SLA)
1:	Initialization: Set the iteration number k=0 so that the initial action selection probability vector for all UAVs is $q_{um}(i) = \frac{1}{M}, \forall u \in, m = \{1, \cdots, M\}$. Have each UAV $u \in U$ randomly select a channel $a_u(0)$ from its optional action set $q(i)$ with equal probability
2:	**while** $\forall q_{um}(i) < 0.99$ **do**
3:	All UAVs broadcast their own status information through the WIFI module, including position, speed, yaw angle, etc
4:	Take other UAVs that can receive information as neighbor UAVs and record them in the neighbor node set J_u
5:	Each UAV selects actions based on channel selection probability
6:	Search on the line segment $l_u = (1 - \lambda)\mathbf{p}_u + \lambda A(a_u)d_{\max}^e$ and record the maximum local mutually beneficial utility function $f_u^{\max}(a_u, a_{J_u})$ and the movement of the UAV $d_u A(a_u(i))$ in the next decision cycle
7:	All UAVs update the action selection probability according to the following rules:
8:	$q_{um}(i+1) = q_{um}(i) + b\widetilde{f}_u(i)[1 - q_{um}(i)], A(m) = a_u(i)$
9:	$q_{um}(i+1) = q_{um}(i) - b\widetilde{f}_u(i)q_{um}(i), A(m) \neq a_u(i)A$
10:	$\widetilde{f}_u(i) = \dfrac{f_u(i)}{U_{\text{cover}} + \sum_{u \in J_u} U_{\text{cover}}}$
11:	**end while**

3.5. Dynamic Deployment Algorithm

Based on the precise potential energy game for each decision cycle described above, we further design a UAV deployment algorithm in a dynamic environment. The specific algorithm is as algorithm 2:

Algorithm 2	Dynamic deployment algorithm
1:	Initialization: Set the deployment area Ω and initial location of the UAV $\mathbf{p}^{init}$, and set the decision time t.
2:	**while** $\eta \leq 0.9$ **do**
3:	Call algorithm 2 to obtain the current optimal movement strategy of the UAV $d_u\mathrm{A}(a_u(t))$ and update the location of each UAV.
4:	$\mathbf{p}_u(t+1) = \mathbf{p}_u(t) + d_u\mathrm{A}(a_u(t))$
5:	Calculate global coverage:
6:	$\eta = \dfrac{\sum_u \sum_s \mathrm{Access}_{U \times S}}{S}$
7:	**end while**

4. Numerical Simulations

4.1. Simulation Environments

In this section, we provide numerical simulation results to evaluate the effectiveness of proposed algorithms. The simulation parameter settings are shown in the Table 1.

Table 1: UAV deployment simulation parameters.

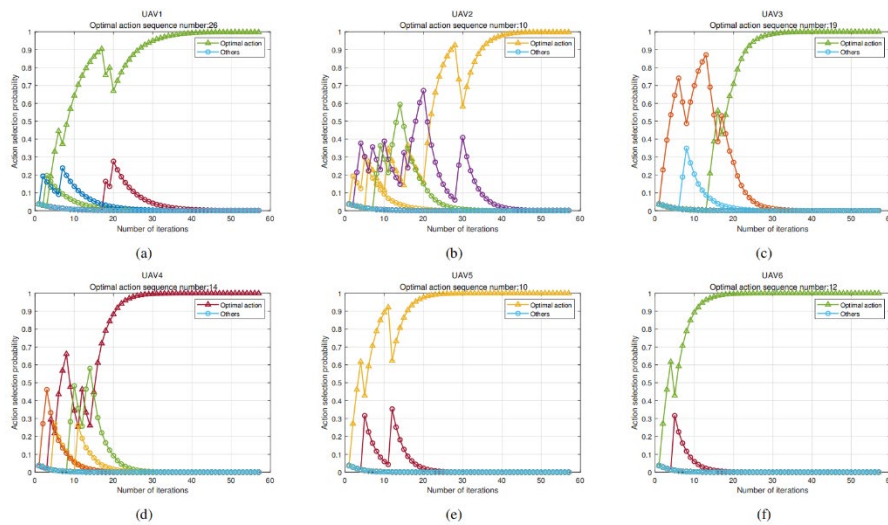| Symbol	Parameter	Value
U	Number of drones	6
U_{cover}	Number of drone connected users	17
Φ	Pitch angle	$\pi/3$
S	Number of sensors	100
p_s	Sensor transmission power	2000 mW
B	Communication channel bandwidth	11 MHz
n_0	Noise power spectral density	-165 dBm/Hz
α	Path loss exponent	2
b	Algorithm learning rate	0.9
$d_{\max}^e$	Maximum exploration distance	250 m

4.2. Simulation Results

Figure 2: Convergence graph of hybrid strategy iteration.

The following figure shows the convergence of the action selection probabilities of six UAVs in their respective action sets. As can be seen from Figure 2, after approximately 40 iterations, the optimal action probability for all UAV hybrid strategy sets converges to 1. At the same time, the action probability curve in the figure also covers the expectation of the automatic learning machine algorithm with the increase of the number of iterations. When the utility brought by a certain action increases, the probability of its selection increases.

Fig. 3 shows the utility function values of UAVs in a decision cycle. The utility function value is the sum of the number of users of the UAV and the number of neighbors. It can be seen from the figure that when the utility values converge to about 25 iterations, this corresponds to the convergence of mixed strategy probabilities, that is, the proposed game model reaches Nash equilibrium. It should be noted that the Nash equilibrium solution obtained by the exploration-based automatic learning machine is the action direction, and the actual deployment position of the autonomous navigation UAV needs to be updated under the constraint of the motion principle and the maximum motion capacity in each deployment decision cycle.
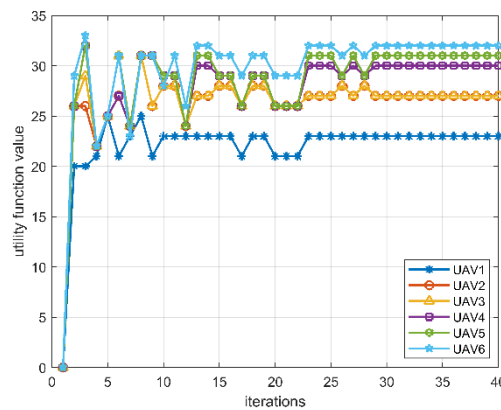

Figure 3: Iterative Convergence Graph of Utility Function Values.

Fig. 4 shows a schematic diagram of the coverage of the real-time deployment of UAVs on a two-dimensional plan. It can be intuitively seen that UAVs are almost evenly distributed in the task area and the users covered are within their maximum number of service users. If the position of the ground sensor changes, the autonomous navigation UAV will also adjust the optimal deployment position based on the real-time perception of the ground sensor information.
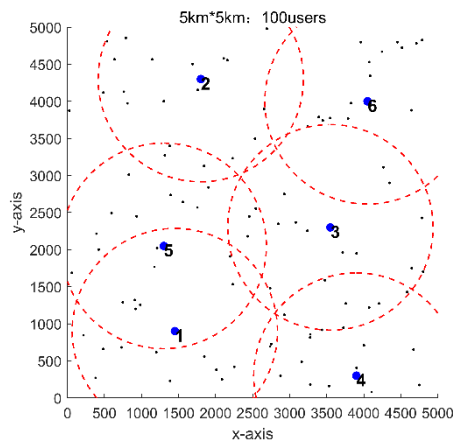

Figure 4: Schematic diagram of drone 2D deployment coverage.

Fig. 5 shows a three-dimensional diagram of the moving waypoints of the real-time deployment of UAVs within each decision cycle. It can be intuitively seen that the UAV is initially placed in the central position of the mission area, obtains the motion direction through the exploration-based automatic learning machine within each deployment decision cycle, and gradually moves to 6 spatially equal directions according to the actual motion ability, which are determined by the Nash equilibrium solution within each deployment cycle. Because the path point selection in each decision space is obtained according to the Nash equilibrium solution of the potential energy game, even if the sensor is moving in

real time, the deployment algorithm can still find the Nash equilibrium solution in each decision cycle. Through continuous iteration, as long as the moving ability of the sensor is weaker than that of the UAV, a stable coverage rate can be achieved. As can be seen from Fig. 5, after several deployment cycles, the autonomous navigation UAV moves to a position that meets the coverage requirements.
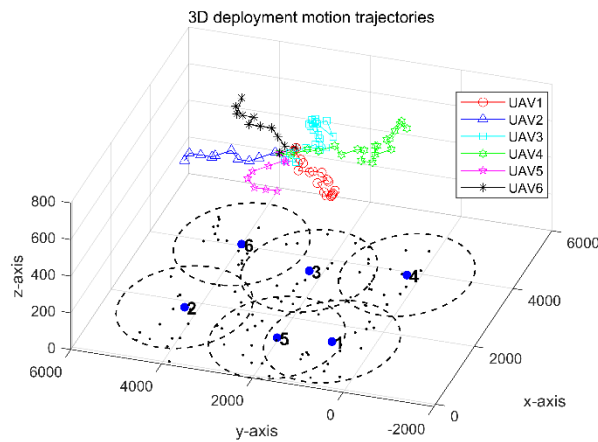

Figure 5: Schematic diagram of drone 3D deployment coverage.

The comparison diagram between the algorithm proposed in this paper and the other algorithm is shown in Fig. 6. After 70 decision cycles, the method proposed in this chapter using the exploratory SLA algorithm and local mutually beneficial utility function can cover more than 90 users, while non exploratory SLA and particle swarm optimization algorithms can cover less than 90 users, while non cooperative SLA algorithms can cover less than 80 users. Through comparison, it can be seen that the proposed 3D deployment algorithm in this paper has better performance.

The comparison diagram between the algorithm proposed in this paper and the other algorithm is shown in Fig. 6. After 70 decision cycles, the method proposed in this chapter using the exploratory SLA algorithm and local mutually beneficial utility function can cover more than 90 users, while nonexploratory SLA and particle swarm optimization algorithms can cover less than 90 users, while non cooperative SLA algorithms can cover less than 80 users. Through comparison, it can be seen that the proposed 3D deployment algorithm in this paper has better performance.
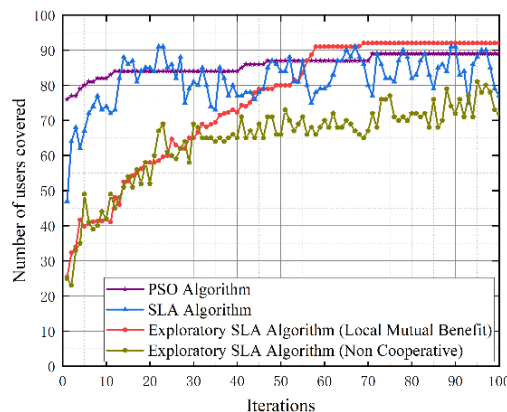

Figure 6: Coverage comparison of different algorithm.

5. Conclusions

In this paper, we proposed a three-dimensional self-organized deployment method for UAVs based on dynamic game models to maximize the service capabilities of UAVs, and we also designed a utility function satisfying potential game conditions. Inspired by SLA, a three-dimensional deployment algorithm for UAVs based on SLA is designed to solve Nash equilibrium. However, we used six UAVs in this simulation, and the ground user was static. If we want to cover dynamic users, how to solve the Nash equilibrium in unknown dynamic environments can be the main difficulties.

References

[1] M. Mozaffari, W. Saad, M. Bennis, and M. Debbah, "Mobile unmanned aerial vehicles (uavs) for energy-efficient internet of things communications," IEEE Transactions on Wireless Communications, vol. PP, no. 11, pp. 7574–7589, 2017.

[2] B. Li, Z. Fei, Y. Zhang, and M. Guizani, "Secure uav communication networks over 5g," IEEE Wireless Communications, vol. 26, no. 99, pp. 114–120, 2019.

[3] Z. Cui, K. Guan, C. Oestges, C. Briso-Rodrıguez, B. Ai, and Z. Zhong, "Cluster-based characterization and modeling for uav air-to-ground time varying channels," IEEE Transactions on Vehicular Technology, vol. 71, no. 7, pp. 6872–6883, 2022.

[4] X. Chen, J. Shi, Z. Yang, and L. Wu, "Low-complexity channel estimation for intelligent reflecting surface-enhanced massive mimo," IEEE Wireless Communications Letters, vol. 10, no. 5, pp. 996–1000, 2021.

[5] D. Yan, K. Guan, D. He, J. Kim, H. Chung, D. Tian, and Z. Zhong, "Blockage effects of road bridge on mmwave channels for intelligent autonomous vehicles," IEEE Transactions on Intelligent Transportation Systems, pp. 1–12, 2023.

[6] K. Guan, H. Yi, D. He, B. Ai, and Z. Zhong, "Towards 6g: Paradigm of realistic terahertz channel modeling," China Communications, vol. 18, no. 5, pp. 1–18, 2021.

[7] H. Jiang, Z. Zhang, C.-X. Wang, J. Zhang, J. Dang, L. Wu, and H. Zhang, "A novel 3d uav channel model for a2g communication environments using aod and aoa estimation algorithms," IEEE Transactions on Communications, vol. 68, no. 11, pp. 7232–7246, 2020.

[8] H. Jiang, Z. Zhang, L. Wu, and J. Dang, "Three-dimensional geometry-based uav-mimo channel modeling for a2g communication environments," IEEE Communications Letters, vol. 22, no. 7, pp. 1438–1441, 2018.

[9] H. Jiang, Z. Zhang, and G. Gui, "Three-dimensional non-stationary wideband geometry-based uav channel model for a2g communication environments," IEEE Access, vol. 7, pp. 26116–26122, 2019.

[10] C. Wei, H. Jiang, J. Dang, L. Wu, and H. Zhang, "Accurate channel estimation for mmwave massive mimo with partially coherent phase offsets," IEEE Communications Letters, vol. 26, no. 9, pp. 2170–2174, 2022.

[11] H. Jiang, B. Xiong, H. Zhang, and E. Basar, "Hybrid far- and near-field modeling for reconfigurable intelligent surface assisted v2v channels: A sub-array partition based approach," IEEE Transactions on Wireless Communications, pp. 1–1, 2023.

[12] B. Xiong, Z. Zhang, J. Zhang, H. Jiang, J. Dang, and L. Wu, "Novel multi-mobility v2x channel model in the presence of randomly moving clusters," IEEE Transactions on Wireless Communications, vol. 20, no. 5, pp. 3180–3195, 2021.

[13] H. Jiang, W. Ying, J. Zhou, and G. Shao, "A 3d wideband two-cluster channel model for massive mimo vehicle-to-vehicle communications in semi-ellipsoid environments," IEEE Access, vol. 8, pp. 23594–23600, 2020.

[14] H. Jiang, Z. Chen, J. Zhou, J. Dang, and L. Wu, "A general 3d non-stationary wideband twin-cluster channel model for 5g v2v tunnel communication environments," IEEE Access, vol. 7, pp. 137 744–137 751, 2019.

[15] H. Jiang, Z. Zhang, L. Wu, J. Dang, and G. Gui, "A 3-d non-stationary wideband geometry-based channel model for mimo vehicle-to-vehicle communications in tunnel environments," IEEE Transactions on Vehicular Technology, vol. 68, no. 7, pp. 6257–6271, 2019.

[16] Y. Guo, X. Li, L. Jia, and Y. Qin, "An efficient rail recognition scheme used for piloting mini autonomous uav in railway inspection," in 2020 International Conference on Sensing, Diagnostics, Prognostics, and Control (SDPC), 2020, pp. 284–290.

[17] H. Jiang, Z. Zhang, L. Wu, and J. Dang, "Novel 3-d irregular-shaped geometry-based channel modeling for semi-ellipsoid vehicle-to-vehicle scattering environments," IEEE Wireless Communications Letters, vol. 7, no. 5, pp. 836–839, 2018.

[18] H. Jiang, Z. Zhang, J. Dang, and L. Wu, "Analysis of semi-ellipsoid scattering channel models for vehicle-to-vehicle communication environments," in 2017 IEEE 85th Vehicular Technology Conference (VTC Spring), 2017, pp. 1–6.

[19] T. Xu, H.-Z. Liu, R. Huang, Z. Yao, and J.-Y. Xu, "Research on motion trajector planning of industrial robot based on ros," in 2022 7th International Conference on Automation, Control and Robotics Engineering (CACRE), 2022, pp. 58–62.

[20] Z. Yu, N. Qi, M. Huo, Z. Fan, and W. Yao, "Fast cooperative trajectory generation of unmanned aerial vehicles using a bezier curve-based shaping method," IEEE Access, vol. 10, pp. 1626–1636, 2022.

[21] M. Radmanesh and M. Kumar, "Grey wolf optimization based sense and avoid algorithm for uav path planning in uncertain environment using a bayesian framework," in 2016 International Conference

on Unmanned Aircraft Systems (ICUAS), 2016.

[22] V. Roberge, M. Tarbouchi, and G. Labonte, "Comparison of parallel genetic algorithm and particle swarm optimization for real-time uav path planning," IEEE Transactions on Industrial Informatics, vol. 9, no. 1, pp. 132–141, 2013.

[23] C. C. Ramirez and C. Briso-Rodr´ıguez, "Diffraction path losses measurements for low altitude uavs," in European Conference on Antennas and Propagation, 2019.

[24] K. Wang, R. Zhang, W. Liang, Z. Zhong, and X. Pang, "Path loss measurement and modeling for low-altitude uav access channels," in 2017 IEEE 86th Vehicular Technology Conference (VTC-Fall), 2018.

[25] Y. Xu, J. Wang, Q. Wu, A. Anpalagan, and Y. D. Yao, "Opportunistic spectrum access in cognitive radio networks: Global optimization using local interaction games," IEEE Journal of Selected Topics in Signal Processing, vol. 6, no. 2, pp. 180–194, 2012.

[26] F. Facchinei and C. Kanzow, "Penalty methods for the solution of generalized nash equilibrium problems," Siam Journal on Optimization, vol. 20, no. 5, pp. 2228–2253, 2010.

[27] P. Sastry, V. Phansalkar, and M. Thathachar, "Decentralized learning of nash equilibria in multi-person stochastic games with incomplete information," IEEE Transactions on Systems, Man, and Cybernetics, vol. 24, no. 5, pp. 769–777, 1994.

[28] A. Rezvanian and M. R. Meybodi, "Finding maximum clique in stochastic graphs using distributed learning automata," International Journal of Uncertainty Fuzziness and Knowledge-Based Systems, vol. 23, no. 1, pp. 1–31, 2015.

[29] F. C. Santos, M. D. Santos, and J. M. Pacheco, "Social diversity promotes the emergence of cooperation in public goods games," Nature, vol. 454, no. 7201, p. 213, 2008.